INTERNATIONAL JOURNAL OF QUANTUM CHEMISTRY, VOL. XXIII, 387-397 (1983)

Force in SCF Theories. First and Second Derivatives of the Potential Energy Hypersurface of Chemical Reaction Systems

H. NAKATSUJI, M. HADA, K. KANDA, AND T. YONEZAWA
Department of Hydrocarbon Chemistry, Faculty of Engineering, Kyoto University, Kyoto, Japan

Abstract

Accurate Hellmann–Feynman force method for the first and second derivatives of energy has been applied to the studies of the chemical reaction systems. We have studied (1) the electronic origins of the structure-reactivity correlations in the reactions $CH_3 + H \rightarrow CH_4$ and $CH_3 + CH_3 \rightarrow C_2H_6$ and (2) the geometries and force constants in the reaction intermediate and the transition state of the reactions $F^- + HF \rightarrow [FHF]^- \rightarrow FH + F^-$ and $H^- + CH_4 \rightarrow CH_4 + H^-$, respectively. An intuitive simplicity of the underlying concepts of the first and second derivatives of the present approach is shown in the analyses.

1. Introduction

The derivatives of a potential energy hypersurface, especially the first and second derivatives, are quantities which play a central role in many fields of theoretical chemistry. In this series of papers [1–5], we are developing a method that is conceptually intuitive and yet numerically accurate, for the studies of the first and second derivatives of a molecule and interacting molecules. Recently, we found a promising method for improving a SCF wave function to satisfy the Hellmann–Feynman theorem [1,2]. It is based on the theorem that states that a sufficient condition for a general SCF wave funtion to satisfy the Hellmann–Feynman theorem is that the basis set includes the derivative $r' = \partial\chi_r/\partial \mathbf{x}_r$ for any basis $r = \chi_r$. We have shown that when the first derivative AO's $\{r'\}$ are added to the original "parent" set r (we call the $\{r,r'\}$ basis as family set), the SCF wave function essentially satisfies the Hellmann–Feynman theorem [1–3]. The validity of this method has been confirmed for closed-shell RHF method [1,3], open-shell RHF and UHF methods [2], and MC-SCF method [2].

When the Hellmann–Feyman theorem is satisfied for the first derivative of energy, an analytic expression of the second derivative of energy becomes much simpler and more intuitive than the straightforward second derivative of the SCF energy [6]. It is given by [4]

$$\frac{\partial^2 E}{\partial X_A \partial Y_B} = \frac{\partial^2 V_{\text{nuc}}}{\partial X_A \partial Y_B} + \sum_{r,s} P_{rs}\delta_{AB} Z_A \langle r| \frac{\partial}{\partial Y_A}\left(\frac{X_A}{r_A^3}\right)|s\rangle + \sum_{r,s} P_{rs} Z_A \left(\left\langle \frac{\partial r}{\partial Y_B}\left|\frac{x_A}{r_A^3}\right| s\right\rangle + \left\langle r \left|\frac{x_A}{r_A^3}\right|\frac{\partial s}{\partial Y_B}\right\rangle\right) + \sum_{r,s}\frac{\partial P_{rs}}{\partial Y_B} Z_A \langle r| \frac{x_A}{r_A^3}|s\rangle, \quad (1)$$

 CCC 0020-7608/83/020387-11$02.10

where

$$\frac{\partial}{\partial Y_A}\left(\frac{x_A}{r_A^3}\right) = \begin{cases}(r_A^2 - 3x_A^2)/r_A^5 + \frac{4}{3}\pi\delta(A), & X_A = Y_A, \\ -3x_A y_A/r_A^5, & X_A \neq Y_A.\end{cases} \quad (2)$$

The first term is a nuclear term. The second term consists of the electric field gradient at nucleus A and the contribution of the density at the nucleus (Fermi term). The third term represents the Hellmann–Feynman force on A due to the AO's displaced by the vibration with keeping the AO coefficients unaltered. The sum of the second and third terms then shows a net effect when the nucleus and AO's associated with it are moved *simultaneously* without changing their AO coefficients (complete following). The last term includes the reorganization of the density matrix due to the vibration (reorganization term). It is a sum of the two terms, i.e., renormalization term and relaxation term [4]. The former arises in order to keep the total wave function normalized during the vibration and the latter arises through the mixing of the virtual orbitals with the occupied orbitals due to molecular vibration.

The present method satisfies the two requirements which seem to be necessary for the theory of the derivatives; one is the numerical accuracy and reliability of the theory, and the other is the conceptual utility of the theory for understanding the electronic origins of the derivatives. Though the energy gradient method [7] has realized the first requirement, it does not fulfill the second one because of an existence of the error term that vanishes identically for a correct SCF wave function.

Here, we report an application of the present method to the study of the force and density origins of the reactions $CH_3 + H \rightarrow CH_4$ and $CH_3 + CH_3 \rightarrow C_2H_6$, and to the second derivative studies of the reaction intermediate and the transition state of the reactions $F^- + HF \rightarrow [FHF]^- \rightarrow FH + F^-$ and $H^- + CH_4 \rightarrow CH_4 + H^-$.

2. Force Method Applied to Chemical Reaction Paths

We apply the new force method to the studies of the force and density origins of the chemical reaction paths of the reactions

$$CH_3 + H \rightarrow CH_4 \quad (3)$$

and

$$CH_3 + CH_3 \rightarrow C_2H_6. \quad (4)$$

We study two different approaches of the methyl group: (a) planar approach in which methyl radical is kept planar throughout the reaction; and (b) angle-optimized approach in which the out-of-plane angle of the methyl group is optimized so that the transverse force acting on the protons of the methyl group vanishes. The C—H length was kept fixed to the equilibrium length of CH_4 and C_2H_6 for reactions (3) and (4), respectively. Previously, we have studied reaction (4) by a semiempirical force method [8].

We have used the family set of the 4-31G set, so that the Hellmann–Feynman theorem is essentially satisfied [3]. For reaction (4), we have used the family set only for the methyl group on the left-hand side. For the counter methyl group, we have used

TABLE I. Heat of reaction along different reaction paths (kcal/mol).

	$CH_3 + H \longrightarrow CH_4$		$CH_3 + CH_3 \longrightarrow C_2H_6$	
	Hartree-Fock	MC-SCF	Hartree-Fock	MC-SCF
Exptl (angle-optimized)	101.6		87	
angle-optimized approach	87.1	93.6	71.6	81.1
planar approach	61.0	73.6	1.9	26.8
difference of two approaches	26.1	20.0	69.7	54.3

the parent set. Since this reaction involves a radical fission, electron correlation is important. We have used the MC-SCF method with the two configurations

$$\Psi_{\text{MC-SCF}} = C_0\Phi_0|\sigma\bar{\sigma}| + C_1\Phi_1|\sigma^*\bar{\sigma}^*|$$

where σ and σ^* denote bonding and antibonding orbitals, respectively, of the C—H or C—C bond. This wave function gives a correct dissociation limit.

Table I gives the heat of reaction calculated for different reaction paths. The experimental value is compared with the result of the angle-optimized approach. The present MC-SCF result is smaller by (7–8)% than the experimental value. The planar approach is much less favorable than the angle-optimized approach. The difference is as large as 20.0 and 54.3 kcal/mol for reactions (3) and (4), respectively. The reaction $CH_3 + CH_3 \rightarrow C_2H_6$ would be almost impossible if the methyl groups were kept planar. The stabilities of CR_3 radicals with large R groups (e.g., triphenyl methyl radical) [9] and of the radicals kept planar experimentally [10] are understood on this basis.

Table II summarizes the geometry of methyl group in the course of the angle-optimized approach, the driving force of the reaction, and its component (F_C and F_H) for the planar approach. For the angle-optimized approach, the forces acting on the protons of CH_3 are very small. Between reactions (3) and (4), reaction (4) occurs at larger separation than reaction (3) as seen from the optimized out-of-plane angle θ and the driving force. In the planar approach, the driving force acting on the CH_3 group becomes smaller than that in the angle-optimized approach, because of the negative

TABLE II. Angle-optimized approach and planar approach in the reactions $CH_3 + H \rightarrow CH_4$ and $CH_3 + CH_3 \rightarrow C_2H_6$.

	Angle-opt approach		Planar approach				Angle-opt approach		Planar approach		
R_{CH} (au)	θ (deg)	driving force (au)	driving force (au)	F_C (au)	$3\times F_H$ (au)	R_{CC} (au)	θ (deg)	driving force (au)	driving force (au)	F_C (au)	$3\times F_H$ (au)
∞	0.0	0.0	0.0	0.0	0.0	∞	0.0	0.0	0.0	0.0	0.0
5.0	4.8	0.015	-	-	-	5.0	5.8	0.042	0.058	0.084	-0.026
4.0	5.8	0.043	0.043	0.053	-0.010	4.0	9.8	0.057	0.016	0.067	-0.051
3.0	13.0	0.075	0.062	0.109	-0.047	2.903	14.0	-0.089	-0.150	0.017	-0.167
2.067	19.47	-0.001	-0.025	0.070	-0.095	2.0	27.0	-0.967	-1.310	-0.951	-0.359
1.5	20.5	-0.501	-0.508	-0.386	-0.122						

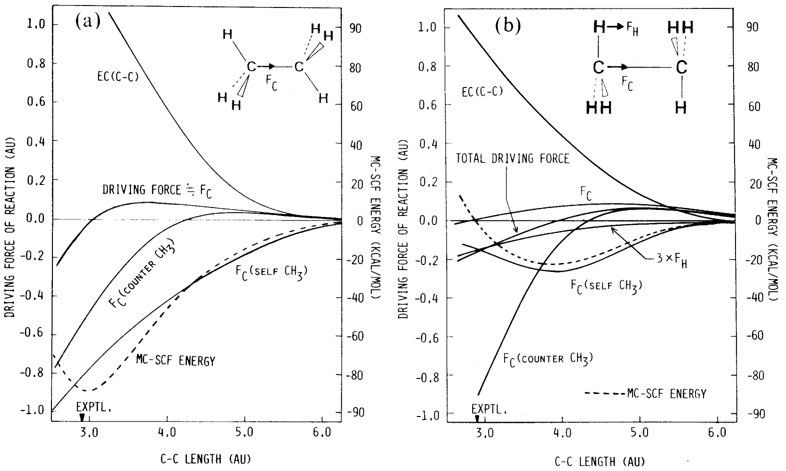

Figure 1. Analysis of the driving force of the reaction $CH_3 + CH_3 \rightarrow C_2H_6$ in the (a) angle-optimized approach and (b) the planar approach. In the angle-optimized approach, the force acting on the protons is very small so that the driving force is nearly equal to the force on carbon F_C. The broken line is the plot of the MC-SCF energy.

forces acting on the terminal protons of CH_3. The force on carbon itself is larger in the planar approach.

In Figure 1, we have compared the analyses of the driving forces in the angle-optimized approach [Fig. 1(a)] and in the planar approach [Fig. 1(b)]. We have partitioned the force acting on the carbon F_C into the EC(C—C) force, F_C(self-CH_3), and F_C(counter-CH_3). The EC(C—C) force is the Hellmann–Feynman force on carbon due to the electron density accumulated in the C—C bond region [11]. (EC denotes exchange.) F_C(self-CH_3) or F_C(counter-CH_3) denotes the Hellmann–Feynman force on carbon due to the electron density and nuclei of the CH_3 group to which the carbon concerned belongs or does not belong, respectively. Figure 1 shows that the EC(C—C) force is a dominant origin of the reaction. It is larger in the angle-optimized approach than in the planar approach. The F_C(counter-CH_3) is small attractive at the beginning but becomes strongly repulsive as the two methyl groups approach closer. It becomes more rapidly repulsive in the planar approach, as expected. The small attractive nature of the F_C(counter-CH_3) is due to the negative gross charge on carbon which attracts

TABLE III. Analysis of the transverse force acting on the terminal protons of methyl radical at the separation $R = 4.0$ a.u. in the planar approach (a.u.).

Reaction	$F_{H\perp}$ total	AD	EC(H-C)	steric repulsion
$CH_3 + H \longrightarrow CH_4$	-0.0032	-0.0013	-0.0005	-0.0014
$2CH_3 \longrightarrow C_2H_6$	-0.0169	-0.0058	-0.0102	-0.0009

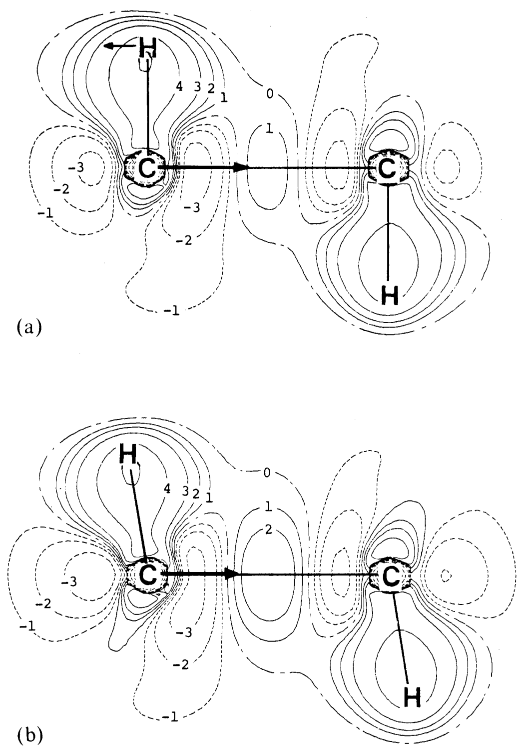

Figure 2. Density difference map at R_{CC} = 4.0 a.u. along the (a) planar and (b) angle-optimized approaches of the reaction $CH_3 + CH_3 \rightarrow C_2H_6$. Because the family set is used only for the methyl group on the left-hand side, the density is slightly nonsymmetric.

the other carbon nucleus. The F_C(self-CH_3) curves are very different between the two approaches. In the angle-optimized approach, the bond density of the C—H bonds bending backward of the carbon pulls it backward. The force increases with increasing bending angle. In the planar approach, the F_C(self-CH_3) would be zero if the electron density of the methyl group were symmetric with respect to the CH_3 plane, as it is in the free methyl radical. The repulsive nature of the F_C(self-CH_3) arises from the outward bent bond of the C—H bond. It pulls the carbon backwards. Since the reaction coordinate of the reaction $CH_3 + CH_3 \rightarrow C_2H_6$ includes an outward bending motion of the C—H bonds, this bent bond is a kind of electron-cloud preceding [12,13] along this reaction. The extent to which it precedes has a maximum near R_{CC} = 4.0 a.u.

Table III shows an analysis of the transverse force $F_{H\perp}$ acting on the terminal protons of the methyl radical in the *planar* approach. The $F_{H\perp}$ is partitioned into the sum of the AD, EC(C—C), and the rest which may be called as "steric repulsion." (AD denotes atomic dipole [11].) The AD and EC(C—C) forces are due to the polarization of the electron density in the atomic and bond regions, respectively, from the plane

TABLE IV. Optimized geometry of FHF^- and CH_5^- (Å).

Calculation	FHF^- ($D_{\infty h}$)	CH_5^- (D_{3h})[a]	
	F-H	$C-H_a$	$C-H_e$
Present 4-31G + first derivatives	1.120	1.700	1.063
Yoshimine, McLean (1967)[b] ($11\sigma_g 9\sigma_u 6\pi_u 5\pi_g$)-STO	1.111		
Almlöf (1972)[c] [4s2p1d/2s1p]	1.123		
Støgård et al. (1975)[d] [4s2p/2s1p]	1.127(HF) 1.140(CI)		
Dedieu, Veillard (1972)[e]		1.737	1.062
Baybutt (1975)[f] [3s2p/2s]		1.735	1.068
Ishida et al. (1977)[g] STO-3G		1.48	1.09
Leforestier (1978)[h] STO-3G+s(H)+3sp(C)		1.70	1.07

[a] H_a and H_e denote axial and equatorial hydrogens, respectively.
[b] Reference 13.
[c] Reference 14.
[d] Reference 15. HF and CI denote Hartree-Fock and configuration interaction values, respectively.
[e] Reference 16.
[f] Reference 17.
[g] Reference 18.
[h] Reference 19.

of the CH_3 group. They reflect the extent of the bent bond [12]. For reactions (3) and (4), the occurrence of the bent bond is an origin of the transverse force $F_{H\perp}$ by 56% and 95%, respectively. Steric repulsion is a minor origin especially in reaction (4).

Figure 2 shows the density difference maps at $R_{CC} = 4.0$ a.u. along the planar and angle-optimized approaches of the reaction $2CH_3 \rightarrow C_2H_6$. We have subtracted the atomic densities from the density of the reacting system. First we discuss the map for the planar approach. When the two methyl radicals, which are planar, are placed face to face at distance 4.0 a.u. apart from each other, the density accumulates in the region midway of the forming C—C bond. This is an electron cloud preceding along the reaction [8,12] and causes the EC(C—C) forces in Figure 1 which is the force origin of the reaction. The accumulation of the density along the C—H bond reflects the existing C—H bond. In finer examination we note that the density along the C—H bond is not symmetric with respect to the C—H axis but bends outward of the C—H axis. This is the bent bond mentioned previously. This is a kind of electron cloud preceding and pulls terminal protons in the direction of the reaction coordinate. The lower

TABLE V. Force constants of the reaction intermediate FHF^- and the transition state CH_5^- (a.u.).

	FHF^-			CH_5^-	
	$Q_1(A_1)$	$Q_2(A_2)$	$Q_3,Q_4(E)$	$Q_1(A_1')$	$Q_2(A_2'')$
Nuclear term	6.171	4.050	-2.006	0.440	0.142
$Z_A \sum P_{rs} \langle r \vert \frac{3x_A^2 - r_A^2}{r_A^5} \vert s \rangle$	5.712	-3.670	1.838	-0.412	-0.089
$Z_A \sum P_{rs} \langle r \vert -\frac{4}{3}\pi\delta(A) \vert s \rangle$	14341.567	33.800	24.846	1.371	79.873
$Z_A \sum P_{rs} \langle r' \vert \frac{x_A}{r_A^3} \vert s \rangle$	-14353.962	-34.134	-24.667	-1.337	-79.888
Total	-0.512	0.045	0.010	0.062	0.038
Renormalization term	2.088	0.498	0.081	0.036	0.181
Relaxation term	-1.222	-0.462	-0.014	-0.043	-0.329
Total	0.866	0.035	0.067	-0.007	-0.148
Grand total	0.354	0.081	0.077	0.055	-0.110

side of Figure 2 is the density when the C—C—H angle is optimized. We note that the C—H bond density becomes almost symmetric with respect to the C—H axis. The accumulation of electron density in the center of the forming C—C bond increases. This explains an increase in the EC(C—C) force shown in Figure 1.

Thus, the force and density origins of reactions (3) and (4) are clarified by the present accurate Hellmann–Feynman force method. The electron cloud preceding into the forming C—C bond and into the backward region of the bending C—H axis are the dominant density origin. The driving force of the reaction has been analyzed with an intuitive force concept. Note that the present result is parallel to that of the previous semiempirical force study [8].

3. Geometry and Force Constant of Reaction Intermediate and Transition State

We study here the geometries and force constants of the reaction intermediate FHF^- of the reaction

$$FH + F^- \rightarrow [FHF]^- \rightarrow F^- + HF, \tag{5}$$

and of the transition state CH_5^- of reaction

$$CH_4 + H^- \rightarrow H^- + CH_4. \tag{6}$$

In Table IV, we have shown the geometry optimized by the present force method. We have used the family set of the 4-31G set so that the Hellmann–Feynman theorem is essentially satisfied [1–3]. The geometry obtained by the present method compares well with the previous results [13–19]. The geometry of the transition state, especially the C—H_a length, seems to be basis set dependent.

Table V shows the force constants and their analyses based on the present approach.

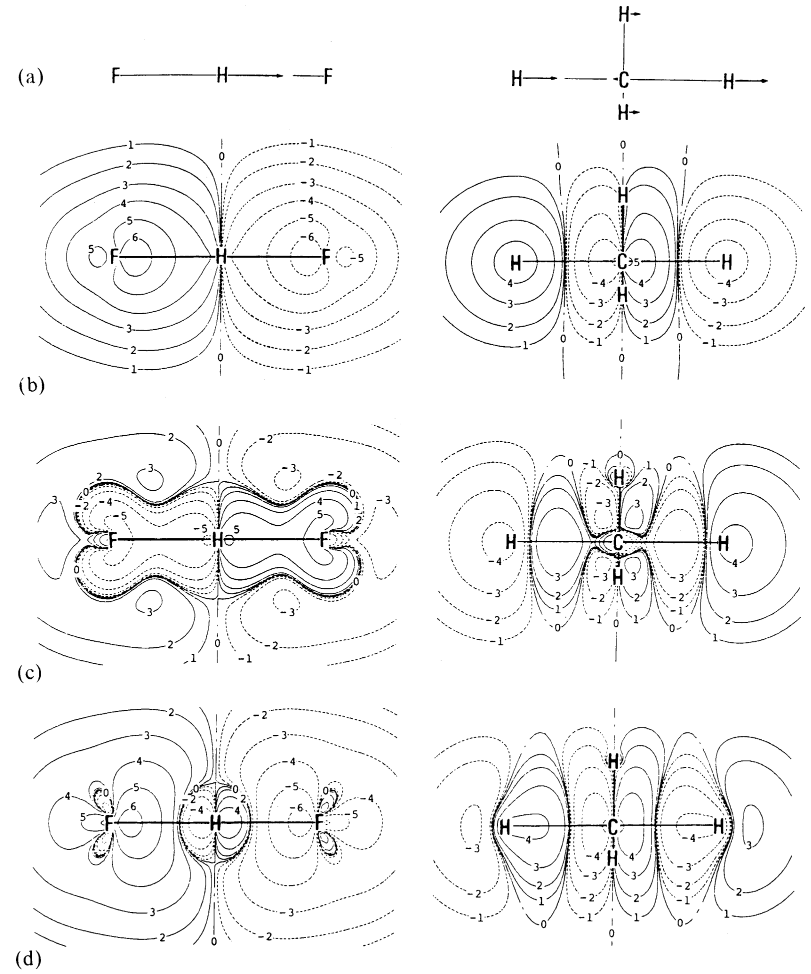

Figure 3. Contour map of the density differential $\sum_{r,s} \partial P_{rs}/\partial Q \chi_r(r)\chi_s(r)$ for the normal mode $Q_2(A_2)$ and $Q_2(A_2'')$ of FHF^- and CH_5^-, respectively. Sketch of (a) the normal mode, (b) the renormalization term, (c) the relaxation term, and (d) the sum of them are shown. The real lines correspond to an increase in density, and the broken lines correspond to a decrease, with the contour values of 0, ±1, ±2, ±3, ±4, ±5, and ±6 corresponding to 0.0, ±0.001, ±0.003, ±0.01, ±0.03, ±0.1, and ±0.3 a.u., respectively.

The contributions of the terms of Eq. (1) are shown. The normal modes are determined by diagonalizing the Hessian matrix. We first discuss the force constants of FHF^-. For FHF^-, there are four modes with A_1, A_2, and E symmetries. They are illustrated as

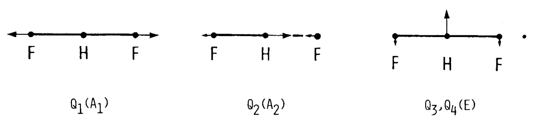

$Q_1(A_1)$ and $Q_2(A_2)$ are the symmetric and antisymmetric stretching modes. The latter is along the reaction path of reaction (5). The bending mode is degenerate. For the stretching modes Q_1 and Q_2, the nuclear term is positive, while for the bending mode, it is negative. The negative contribution is understood from the definition of the bending force constant

$$-\lim_{\Delta\theta\to 0} \frac{[F(\theta+\Delta\theta)-F(\theta)]_\perp}{R_{HF}\cdot\Delta\theta}\,.$$

Though the internuclear repulsion between H and F is always parallel to the HF bond, the vector $F(\theta + \Delta\theta) - F(\theta)$ has a component perpendicular to the bond and gives a negative contribution to the force constant. The same was true in the bending mode of H_2O [4]. In the next three terms (complete following term), the Fermi and displaced AO terms are very large, because of a large inner-shell contribution. This is especially so for the $Q_1(A_1)$ mode because there the moving nuclei are fluorines. However, these terms cancel. The sum of the nuclear and complete following terms is negative for the $Q_1(A_1)$ mode, in which the moving nucleus is fluorines, and positive for the $Q_2(A_2)$ and Q_3, $Q_4(E)$ modes, in which the moving nucleus is mainly hydrogen. The next three terms show the effect of reorganization of the electron density matrix due to the vibration. The renormalization term is always positive, but the relaxation term is negative. The sum is positive, showing that the renormalization term is larger than the relaxation term. At the bottom, the calculated force constants are given. We see that the force constant of the antisymmetric stretching mode $Q_2(A_2)$ is very small in comparison with that of the symmetric stretching mode $Q_1(A_1)$. It is close to the force constant of the bending mode Q_3, $Q_4(E)$. For most stable AB_2 molecules, the force constants of the corresponding two modes are similar. This result is reasonable considering that the Q_2 mode is along the reaction coordinate of reaction (5).

In Figure 3, we hve shown the density differential map for the $Q_2(A_2)$ mode of the FHF^- molecule (left-hand side). The renormalization term shows a typical behavior of the electron cloud incomplete following [12,20]. The density flows in the reverse direction of the nuclear motion. On the other hand, the relaxation term shows a beautiful pattern of the electron cloud preceding. The density accumulates in front of the nuclei H and F in the direction of the motion. It pulls the nuclei in the direction of the nuclear motion and then gives negative contribution to the force constant. The total sum reflects mainly the renormalization term except for a small region near the proton.

We next consider the force constants of the transition state CH_5^-. The normal modes of CH_5^- consist of 12 modes (two A_1', two A_2'', six E', and two E'' modes). Among these, one normal mode has a negative force constant and all others have positive ones. Here, we give an analysis of the force constant for the A_1' and A_2'' modes. They are illustrated as

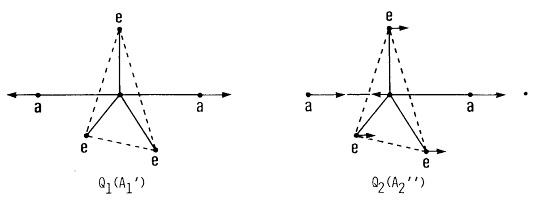

$Q_1(A_1')$ is a totally symmetric vibration of the C—H bonds. $Q_2(A_2'')$ is the so-called reaction coordinate involving Walden inversion. In Table V, the sum of the nuclear term and the complete following term is positive as usually is for hydride molecules. The reorganization term shows an interesting characteristics of the transition state. Though the signs of the renormalization and relaxation terms are positive and negative, respectively, as is usual, the relaxation term is larger here than the renormalization term, giving a net negative contribution of the reorganization term. In the reaction coordinate $Q_2(A_2'')$, this is an origin of the *negative* force constant. In the coordinate $Q_1(A_1')$, the final force constant is positive, however, since the sum of the nuclear and complete following terms gives a larger positive contribution.

Characteristic behavior of the electron density along the reaction coordinate is seen in the density differential map shown on the right-hand side of Figure 3. The relaxation term shows a typical pattern of the electron cloud preceding. The density increases in the direction of the reaction coordinate in all the regions near the moving nuclei H_a, H_e, and C. The relaxation term shows a characteristics of the electron cloud incomplete following in the neighborhood of H_a and C. Near H_e, the renormalization term also shows the nature of the electron cloud preceding. In the total sum, the relaxation contribution surpasses the renormalization contribution, showing a beautiful pattern of the electron cloud preceding. This is a density origin of the *negative* force constant of the reaction coordinate $Q_2(A_2'')$.

4. Conclusion

Here, we have shown some applications of the accurate Hellmann–Feynman force method to the studies of the first and second derivatives of the potential energy hypersurface of the reacting systems. We have studied the electronic origins of the driving force of the chemical reaction and the geometries and force constants of the reaction intermediate and transition state. The intuitive simplicity of the underlying concepts of the first and second derivatives of the present approach, and the accuracy of the calculated results, would be useful in studying the nature of the variety of chemical reactions.

Bibliography

[1] H. Nakatsuji, K. Kanda, and T. Yonezawa, Chem. Phys. Lett. **75**, 340 (1980).
[2] H. Nakatsuji, T. Hayakawa, and M. Hada, Chem. Phys. Lett. **80**, 94 (1981).
[3] H. Nakatsuji, K. Kanda, M. Hada, and T. Yonezawa, J. Chem. Phys. **77**, 3109 (1982).
[4] H. Nakatsuji, K. Kanda, and T. Yonezawa, J. Chem. Phys. **77**, 1961 (1982).
[5] H. Nakatsuji and K. Kanda, in *Local Density in Quantum Chemistry and Solid State Theory*, J. Avery and J. P. Dahl, Eds. (Plenum Press, New York, 1982), to appear.
[6] J. A. Pople, R. Krishnan, H. B. Schlegel, and J. S. Binkley, Int. J. Quantum Chem. Quantum Chem. Symp. **13**, 225 (1979).
[7] P. Pulay, in *Modern Theoretical Chemistry*, H. F. Schaefer III, Ed. (Plenum, New York, 1977), Vol. 4, Chap. 4.
[8] H. Nakatsuji, T. Kuwata, and A. Yoshida, J. Am. Chem. Soc. **95**, 6894 (1973).
[9] D. J. Nonhebel and J. C. Walton, *Free-Radical Chemistry* (Cambridge, U.P., London, 1974), p. 110.

[10] O. Neunhoeffer and H. Haasse, Chem. Ber. **91,** 1801 (1958).
[11] H. Nakatsuji, J. Am. Chem. Soc. **95,** 345 (1973); **95,** 354 (1973).
[12] H. Nakatsuji, J. Am. Chem. Soc. **95,** 2084 (1973); **96,** 24 (1974); **96,** 30 (1974).
[13] M. Yoshimine and A. D. McLean, Int. J. Quantum Chem. Quantum Chem. Symp. **1,** 313 (1967).
[14] J. Almlöf, Chem. Phys. Lett. **17,** 49 (1972).
[15] A. Støgård, A. Strich, J. Almlöf, and B. Roos, Chem. Phys. **8,** 405 (1975).
[16] A. Dedieu and A. Veillard, J. Am. Chem. Soc. **94,** 6730 (1972).
[17] P. Baybutt, Mol. Phys. **29,** 389 (1975).
[18] K. Ishida, K. Morokuma, and A. Komornicki, J. Chem. Phys. **66,** 2153 (1977).
[19] C. Leforestier, J. Chem. Phys. **68,** 4406 (1978).
[20] H. Nakatsuji and T. Koga, in *The Force Concept in Chemistry*, B. M. Deb, Ed. (Van Nostrand-Reinhold, New York, 1981), Chap. 3.